ploited for shikimate analysis except for the HPLC conditions employed (semiprep Whatman Partisil-10 SAX; 80:20 water/acetonitrile, 7.5 mM phosphate buffer, pH 2.4). Typically the recovery of radiolabeled shikimate or DAH was 75–80% after extraction, workup, and separation by anion-exchange high-pressure liquid chromatography. Values for DAH and shikimate accumulation were corrected for radiolabel lost during the analysis.

Acknowledgment. Work was supported by a generous grant from the Herman Frasch Foundation and a Du Pont Young Faculty Grant.

Registry No. 1a, 105103-72-8; **2b**, 118377-79-0; DHQ synthase, 37211-77-1; 3-deoxy-D-*arabino*-heptulosonic acid 7-phosphate, 2627-73-8.

Studies of Protein Hydration in Aqueous Solution by Direct NMR Observation of Individual Protein-Bound Water Molecules†

Gottfried Otting and Kurt Wüthrich*

Contribution from the Institut für Molekularbiologie und Biophysik, Eidgenössische Technische Hochschule-Hönggerberg, CH-8093 Zürich, Switzerland. *Received June 24, 1988*

Abstract: Proton nuclear magnetic resonance was used to study individual molecules of hydration water bound to the protein basic pancreatic trypsin inhibitor (BPTI) in aqueous solution. The experimental observations are nuclear Overhauser effects (NOE) between protons of individual amino acid residues of the protein and those of sufficiently tightly bound water molecules. These NOEs were recorded by two-dimensional nuclear Overhauser enhancement spectroscopy (NOESY) in the laboratory frame, and by the corresponding experiment in the rotating frame (ROESY). The detection of NOEs with water protons was enabled by a solvent suppression technique which provides a uniform excitation profile in NOESY and ROESY, except at the ω_2 frequency of the water signal. From NOESY and ROESY spectra recorded at 5, 36, 50, and 68 °C, intermolecular ^1H-^1H NOEs between the protein and four water molecules buried in its interior were individually assigned, and additional NOEs between surface residues of the protein and labile protons with the chemical shift of the bulk water were identified. For the hydration waters that can be observed by NOEs at 36 °C, an upper limit for the proton-exchange rate with the bulk water is estimated to be 3×10^9 s^{-1}. These NOE-observable water molecules account only for a small percentage of the hydration waters seen in the crystal structure of BPTI. This observation supports the independently established picture of increased disorder near the molecular surface in protein structures in solution.

Three-dimensional protein structures can nowadays be determined either by X-ray diffraction in single crystals or by nuclear magnetic resonance (NMR)[1] in solution.[2] High-resolution crystal structures of globular proteins include typically numerous water molecules in defined hydration sites.[3,4] In aqueous solution, evidence for the presence of protein-bound hydration water could also be established, but the experiments used so far could not provide observations on individual molecules of hydration water. For example, measurements of the relaxation enhancement on the water signal in aqueous protein solutions led to the conclusion that the observed magnetization transfer is not only a consequence of chemical exchange between water protons and labile protons of the protein, but occurs also via cross relaxation at the water–protein interface.[5] In different experiments, pH-independent transfer of magnetization to slowly exchanging protein protons was observed upon irradiation of the water resonance in protein solutions.[6] In these experiments the observation of negative nuclear Overhauser effects (NOE)[6] showed that there must be hydration water bound with lifetimes that are comparable with the overall rotational correlation time of the hydrated protein, which is of the order of nanoseconds. Evidence for the presence, in certain proteins, of a small number of hydration waters that exchange with the bulk water on a time scale of seconds was deduced from ^{18}O tracer experiments.[7] None of these solution experiments could, however, provide information on the location of the hydration sites in the protein. The present paper describes a NMR technique that is capable of identifying individual molecules of hydration water and characterizing their binding sites on the protein molecule.

Our interest in detailed studies of protein hydration in solution was revived by recent observations with the protein Tendamistat, for which high-resolution structures were determined by NMR in solution and in single crystals.[8] Even though the global molecular architectures in the two states are very nearly identical, significant structural differences were identified near the protein surface. There is also evidence that compared to the core of the protein, the increase of structural disorder near the molecular surface is more pronounced in solution than in the crystals.[8] The experiments described in the present paper now demonstrate by observations with individual water molecules that in solution the hydration network on the protein surface is kinetically highly labile. Evidence for mobile hydration waters in water–protein systems

† This paper was presented at the 4th International Symposium on Biological and Artificial Intelligence Systems, Trento, Italy, September 18–22, 1988.

(1) Abbreviations and symbols used: NMR, nuclear magnetic resonance; NOE, nuclear Overhauser enhancement; ROE, rotating-frame Overhauser enhancement; 2D, two-dimensional; NOESY, two-dimensional nuclear Overhauser enhancement spectroscopy in the laboratory frame; ROESY, two-dimensional nuclear Overhauser enhancement spectroscopy in the rotating frame; ω_0, Larmor frequency; τ_c, rotational correlation time.

(2) Wüthrich, K. *NMR of Proteins and Nucleic Acids*; Wiley: New York, 1986.

(3) Deisenhofer, J.; Steigemann, W. *Acta Crystallogr., Sect. B* **1975**, *31*, 238.

(4) (a) Blundell, T. L.; Johnson, L. N. *Protein Crystallography*; Academic Press: New York, 1976. (b) Teeter, M. M. *Proc. Natl. Acad. Sci. U.S.A.* **1984**, *81*, 6014.

(5) Koenig, S. H.; Bryant, R. G.; Hallenga, K.; Jacob, G. S. *Biochemistry* **1978**, *17*, 4348.

(6) Stoesz, J. D.; Redfield, A. G.; Malinowksi, D. *FEBS. Lett.* **1978**, *91*, 320.

(7) Tüchsen, E.; Hayes, J. M.; Ramaprasad, S.; Copie, V.; Woodward, C. *Biochemistry* **1987**, *26*, 5163.

(8) (a) Kline, A. D.; Braun, W.; Wüthrich, K. *J. Mol. Biol.* **1986**, *189*, 377. (b) Kline, A. D.; Braun, W.; Wüthrich, K. *J. Mol. Biol.* **1988**, *204*, 675. (c) Pflugrath, J.; Wiegand, E.; Huber, R.; Vertesy, L. *J. Mol. Biol.* **1986**, *189*, 383.

0002-7863/89/1511-1871$01.50/0

was previously also derived from measurements of NMR relaxation times and line widths,[9] which could, however, only provide a global view.

General Considerations on the Observation of Individual Molecules of Hydration Water by ^{1}H NMR

One can anticipate that the proton chemical shifts of protein-bound water molecules are influenced by the protein environment in a similar fashion as those of the individual amino acid residues upon incorporation into a globular protein structure.[2] On the basis of the resulting unique chemical shifts for different individual hydration waters, direct observation of distinct ^{1}H NMR lines corresponding to these water molecules should in principle be possible and thus provide direct evidence for their presence. In practice, however, it appears that as a rule the proton resonances of protein hydration water in aqueous solution are at the same chemical shift as the bulk water. From this one must conclude either that the effects of protein binding on the water chemical shifts are too small to be resolved, which would impose an upper limit of ca. 0.05 ppm on these shifts, or that exchange of protons from hydration water with the bulk water averages out the differences in chemical shift induced by the chemical nature of the hydration sites. This latter explanation applies for nearly all hydroxyl and carboxylate protons of the amino acid side chains of Ser, Thr, Tyr, Asp, and Glu in proteins, for which it is well-known that they have intrinsically different chemical shifts from that of H_2O.[2] Different time scales govern the averaging of the chemical shifts and the spin relaxation processes that lead to the appearance of NOEs.[2] In the situation where the resonance lines of both the OH groups of the protein and the hydration waters are merged with that of the bulk water, one may therefore still observe individual molecules of hydration water through specific intermolecular NOEs.

The degeneracy of all water proton and most hydroxyl proton chemical shifts requires that complete ^{1}H NMR assignments are available for the protein, and that the solution structure of the protein is known at high resolution, before unambiguous assignments of NOEs between protons of the protein and hydration water molecules can be obtained. In addition, one must rule out that the observed effects arise from chemical exchange of protons, and that the interactions could be with OH groups of the protein rather than with protein-bound water molecules.

Distinction between different possible mechanisms of intermolecular magnetization transfer can be based on differences in qualitative aspects of two-dimensional nuclear Overhauser experiments in the rotating frame (ROESY). A negative sign of a ROESY cross peak relative to the diagonal peaks shows that the magnetization transfer is by direct cross relaxation, since both transfer by first-order spin diffusion pathways or by chemical exchange lead to positive cross peaks.[10] On the other hand, ROESY spectra may contain extra peaks due to homonuclear Hartmann–Hahn transfer,[11] and the cross peak intensities have to be corrected for off-resonance effects in the ROESY spin lock.[12] As a control, comparisons with nuclear Overhauser enhancement experiments in the laboratory frame (NOESY) can therefore be helpful. In the present experiments we further used studies of the effects of temperature variation on the NOESY and ROESY spectra to identify cross peak intensity arising from chemical exchange. Once a cross peak between a protein proton and a proton at the bulk water chemical shift has thus been demonstrated to correspond to a direct NOE, distinction between intermolecular NOEs with hydration water and intramolecular NOEs with OH groups can only be achieved on the basis of the solution structure of the protein, from which the location of all the side-chain hydroxyl and carboxylate groups is known. Thereby we used as a criterion for the identification of a NOE with a hydration water molecule that the interacting protein proton must be at a distance of at least 4.0 Å from the nearest OH group; otherwise the distinction between hydration water and hydroxyl groups would remain undecided. Along similar lines, a distinction may be made between the two situations that either one molecule of hydration water interacts with two neighboring groups of protein protons or that two different water molecules interact with different protein protons, which are located far apart in the structure.

NMR experiments enable one to estimate limits on the lifetimes of the hydration water protons with respect to exchange in and out of the protein hydration sites. A lower limit can be obtained from the observation that the chemical shift is averaged with that of the bulk water by using an assumed value for the protein-induced chemical shift. For example, with the assumption that the protein-induced shift amounts to 0.02 ppm, observation of a single, averaged water resonance at a Larmor frequency of 600 MHz would indicate that the exchange rate is faster than 80 s^{-1}. An upper limit may be derived by using the fact that NOESY cross peaks manifesting direct NOEs are positive (i.e., the NOE has a negative sign) if the effective correlation time, τ_c, is longer than $1.12\omega_o^{-1}$, where ω_o is the Larmor frequency. Otherwise the NOESY cross peak would be negative. In practice, NOESY cross peaks manifesting NOEs (rather than proton exchange) will have significant intensity only for $\tau_c \gg 1.12\omega_o^{-1}$, whereas for $\tau_c \lesssim 1.12\omega_o^{-1}$ NOEs are more easily observed in ROESY experiments.[10]

NMR Experiments for Direct Observation of Individual Hydration Water Molecules

Commonly protein ^{1}H NMR spectra are recorded either in ^2H_2O solution or in H_2O solution with selective saturation to suppress the solvent resonance.[2] Such experiments do a priori preclude observation of hydration water. Alternative solvent suppression techniques that do not eliminate the water signal during the preparation period[13,14] have been used in studies of nucleic acids,[15-19] where the resonances of the labile protons would be suppressed by the saturation technique.[2] For work with proteins these solvent suppression schemes have rarely been used, since they have the disadvantage of nonuniform spectral excitation profiles along the ω_2 axis,[15-18] or along both ω_1 and ω_2[19] in 2D NMR experiments. However, with the use of recent advances in instrumentation, in particular digital phase shifters and fast switches for changing the radio-frequency power settings, selective pulses of controlled phase can now be applied to the water resonance, and it is possible to selectively eliminate the water signal within milliseconds immediately before the detection period.[20] The resulting spectra have a uniform excitation profile in both dimensions, except for a narrow spectral region parallel to the ω_1 axis at the ω_2 frequency of the water signal, which would be obscured by t_1 noise from the residual water signal also in spectra recorded with solvent presaturation.[2] For studies of hydration waters we employed a variant of an experiment proposed by Sklenář and Bax.[20] Figure 1 shows the pulse sequences applied for recording NOESY and ROESY spectra in H_2O, whereby the water signal is suppressed only at the end of the mixing time.

In NOESY experiments (Figure 1A) with $\tau_m \gtrsim 100$ ms, the water magnetization is, as a result of radiation damping,[18,21] mainly aligned along the z axis at the moment when the first selective pulse, $(\pi/2)_\theta$, is applied. For shorter mixing times a homospoil

(9) (a) Kuntz, I. D., Jr.; Kauzmann, W. *Adv. Protein Chem.* **1974**, *28*, 239. (b) Halle, B.; Andersson, T.; Forsēn, S.; Lindman, B. *J. Am. Chem. Soc.* **1981**, *103*, 500. (c) Shirley, W. M.; Bryant, R. G. *J. Am. Chem. Soc.* **1982**, *104*, 2910. (d) Polnaszek, C. F.; Bryant, R. G. *J. Chem. Phys.* **1984**, *81*, 4038.

(10) Bothner-By, A. A.; Stephens, R. L.; Lee, J. *J. Am. Chem. Soc.* **1984**, *106*, 811.

(11) Neuhaus, D.; Keeler, J. *J. Magn. Reson.* **1986**, *68*, 568.

(12) Griesinger, C.; Ernst, R. R. *J. Magn. Reson.* **1987**, *75*, 261.

(13) Redfield, A. G.; Gupta, R. K. *J. Chem. Phys.* **1971**, *54*, 1418.

(14) Hore, P. J. *J. Magn. Reson.* **1983**, *55*, 283.

(15) Kearns, D. R.; Mirau, P. A.; Assa-Munt, N.; Behling, R. W. In *Nucleic Acids: The Vectors of Life*; Pullman, B., Jortner, J., Eds.; D. Reidel Publishing Co.: Dordrecht, The Netherlands, 1983; pp 113–125.

(16) Hilbers, C. W.; Heerschap, A.; Haasnoot, C. A. G.; Walters, J. A. L. I. *J. Biomol. Struct. Dyn.* **1983**, *1*, 183.

(17) Boelens, R.; Scheek, R. M.; Dijkstra, K.; Kaptein, R. *J. Magn. Reson.* **1985**, *62*, 378.

(18) Bax, A.; Sklenář, V.; Clore, G. M.; Gronenborn, A. M. *J. Am. Chem. Soc.* **1987**, *109*, 6511.

(19) Otting, G.; Grütter, R.; Leupin, W.; Minganti, C.; Ganesh, K. N.; Sproat, B. S.; Gait, M. J.; Wüthrich, K. *Eur. J. Biochem.* **1987**, *166*, 215.

(20) Sklenář, V.; Bax, A. *J. Magn. Reson.* **1987**, *75*, 378.

(21) Abragam, A. *The Principles of Nuclear Magnetism*; Oxford University Press: New York, 1961.

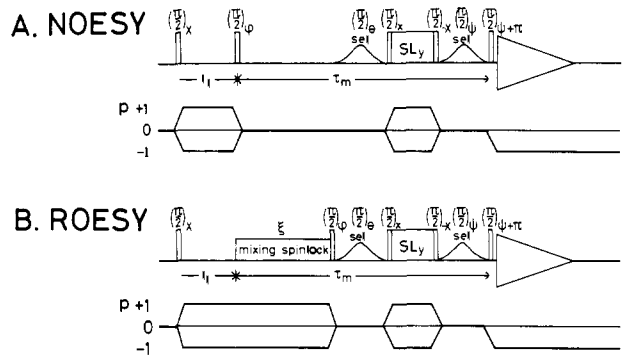

Figure 1. Pulse sequences used for the observation of intermolecular NOEs between water protons and protein protons by NOESY or ROESY, where SL denotes spin-lock pulses, t_1 and τ_m are the evolution period and the mixing time, and the observation period t_2 is indicated by a schematic free induction decay. The desired coherence transfer pathways shown below the pulse sequences are obtained by the following phase cycling: (A) NOESY: $\varphi = x, x, -x, -x, x, x, -x, -x$; $\theta = x, -x, x, -x, x, -x, x, -x$; $\psi = x, x, x, x, -x, -x, -x, -x$; receiver = $x, x, -x, -x, -x, -x, x, x$. Additional incrementation of the phases of all pulses and of the receiver in steps of 90° (CYCLOPS) results in a 32-step phase cycle. (B) ROESY: same as (A), except for the addition that, independent of all other phase, ξ is cycled between $-y$ and $+y$ after each package of eight scans, so that a 64-step phase cycle is obtained.

pulse can be used immediately before this first selective pulse to dephase all transverse magnetization present. The selective 90° pulse turns the longitudinal water magnetization vector into the transverse plane, from where it is immediately turned back to the z axis by the following nonselective $(\pi/2)_x$ pulse. The protein magnetization of interest, which is not excited by the selective pulse, is at that point aligned along the y axis. The following spin-lock pulse with phase y, SL_y, then locks the protein y magnetization and destroys with its radio-frequency inhomogeneity all coherences in the xz plane, which originate primarily from H_2O. The subsequent nonselective $(\pi/2)_{-x}$ pulse brings the spin-locked y magnetization, which contains the protein magnetization and residual contributions from H_2O, back to the z axis. The subsequent combination of a selective 90° pulse on the water resonance, $(\pi/2)_\psi$, and the nonselective pulse $(\pi/2)_{\psi+\pi}$ select again for protein z magnetization and convert it into observable coherence. In ROESY (Figure 1B), the mixing spin-lock period is followed by a $\pi/2$ pulse with its phase shifted by 90° relative to the phase of the spin lock. The spin-locked magnetization is thus turned to the z axis, and the same solvent suppression scheme as in the NOESY experiment of Figure 1A is then applied to the longitudinal magnetization. The following phase cycling is used with the pulse sequences for both NOESY and ROESY. Coherences of even order are selected during the mixing time by phase cycling of φ and ψ.[22] The spin-lock pulse, SL_y, further suppresses all multiple-quantum coherences. Cycling of the phase θ suppresses dispersive tails of the residual water signal. Axial peaks are shifted to the periphery of the spectrum by the use of time-proportional phase incrementation (TPPI).[22]

In the coherence transfer pathway of the ROESY experiment of Figure 1B, coherence order 0 is present during the water purging sequence following the mixing spin-lock. Therefore, longitudinal relaxation via NOE may occur during the selective pulses. However, since for macromolecules the buildup rate of rotating-frame Overhauser effects (ROE) is twice as fast as the NOE buildup, and ROEs have opposite sign to that of NOEs,[12] the ROE is expected to dominate the NOE for mixing spin-lock periods equal to or longer than a selective 90° pulse.

Finally, it should be pointed out that for instruments where homospoil pulses are available, the pulse schemes of Figure 1 can be modified so as to achieve the same favorable excitation profile without the spin-lock purge pulse SL_y. In practice, a 2-ms spin-lock was found to be sufficiently long for efficient purging of the solvent resonance and at the same time sufficiently short so that the extent of coherent transfer of magnetization during the spin-lock period is negligible. Such deleterious effects by the spin-lock are obviously completely avoided if the $(\pi/2)_x$-SL_y-$(\pi/2)_{-x}$ sequence is replaced by a homospoil pulse.

Results and Discussion

A series of NOESY and ROESY spectra recorded at 5, 36, 50, and 68 °C were used to assign the cross peaks between protein resonances and the water signal. Figures 2 and 3 are representative of the results obtained. Figure 2 shows contour plots of regions including the water resonance which were taken from NOESY spectra at 4 and 68 °C recorded with the pulse sequence of Figure 1A. At 4 °C the water resonance is at 5.01 ppm. Since there are no BPTI resonances at the same chemical shift,[27] all cross peaks seen at $\omega_1 = 5.01$ ppm must manifest interactions of protons from the protein with protons at the chemical shift of the water resonance. At 68 °C the water resonance is shifted to 4.45 ppm and overlaps with some protein lines, e.g., the α-protons of Lys-15 and Lys-46.[27] At this temperature some of the cross peaks at the ω_1 frequency of the water signal may therefore represent intramolecular NOEs with these α-protons rather than NOEs with water molecules or hydroxyl groups. Figure 3 shows that with few exceptions the same cross peaks at the ω_1 frequency of H_2O are observed by NOESY and ROESY in the ω_2 range from 6 to 10 ppm. The negative peak intensities seen in ROESY for the cross peaks between amide protons and the water line document that the magnetization transfer by ROE is more efficient than the chemical exchange of most of these protons in the temperature range 5–50 °C. At 5 °C positive ROESY cross peaks due to chemical exchange are observed for the side-chain amino protons of lysine residues and for a singlet resonance at 10.07 ppm, which was assigned to the side-chain hydroxyl proton of Tyr-35[28] by its NOEs to the 3,5 ring protons of Tyr-35, $C^\alpha H$ of Cys-38, and NH and β-CH_3 of Ala-40, which are all near neighbors of the Tyr-35 hydroxyl group in both the crystal structures of BPTI[3,29,30] and the solution structure determined by NMR.[31] Upon variation of the temperature from 5 to 68 °C, which is approximately 20 °C below the denaturation temperature of BPTI, the position and the intensity of the exchange peaks of the lysine amino protons change as they approach the coalescence temperature with the solvent resonance. Similarly, at 68 °C the OH resonance of Tyr-35 is broadened and shifted toward the water resonance. At 68 °C positive ROESY exchange cross peaks are seen also for several amide protons, and exchange cross peaks for the guanidino protons of arginine residues start to appear at 36 °C. The exchange peaks of the amide protons of Lys-46, Arg-39, Thr-11, Asp-3, and Glu-49 are identified in Figure 2. All the exchange peaks observed at 68 °C are from amide protons that were previously found to exchange too rapidly to be seen in a COSY spectrum recorded in ^2H_2O at 10 °C and pH 3.6 immediately after sample preparation[32,33] and are therefore among the most labile amide protons in BPTI.

(22) Ernst, R. R.; Bodenhausen, G.; Wokaun, A. *Principles of Nuclear Magnetic Resonance in One and Two Dimensions*; Clarendon, Oxford, 1987.
(23) Kessler, H.; Griesinger, C.; Kerssebaum, R.; Wagner, K.; Ernst, R. R. *J. Am. Chem. Soc.* **1987**, *109*, 607.
(24) Morris, G. A.; Freeman, R. *J. Magn. Reson.* **1978**, *29*, 433.
(25) Bauer, C.; Freeman, R.; Frenkiel, T.; Keeler, J.; Shaka, A. J. *J. Magn. Reson.* **1984**, *58*, 442.
(26) Shinnar, M.; Leigh, J. S. *J. Magn. Reson.* **1987**, *75*, 502.
(27) ^1H NMR assignments for BPTI are available at 36 °C (ref 31) and 68 °C (Wagner, G.; Wüthrich, K. *J. Mol. Biol.* **1982**, *155*, 347.) The presently used assignments at different temperatures and pH were established by comparison with these data.
(28) This resonance was not assigned previously, since it was not observed in the spectra recorded with water presaturation.
(29) Wlodawer, A.; Walter, S.; Huber, R.; Sjölin, L. *J. Mol. Biol.* **1984**, *180*, 301.
(30) Wlodawer, A.; Nachman, J.; Gilliland, G. L.; Gallagher, W.; Woodward, C. *J. Mol. Biol.* **1987**, *198*, 469.
(31) Wagner, G.; Braun, W.; Havel, T. F.; Schaumann, T.; Gō, N.; Wüthrich, K. *J. Mol. Biol.* **1987**, *196*, 611.
(32) Wagner, G.; Wüthrich, K. *J. Mol. Biol.* **1982**, *160*, 343.
(33) The assignments of Ile-19 and Asp-3 given in ref 32 must be interchanged: Tüchsen, E.; Woodward, C. *J. Mol. Biol.* **1985**, *185*, 405.

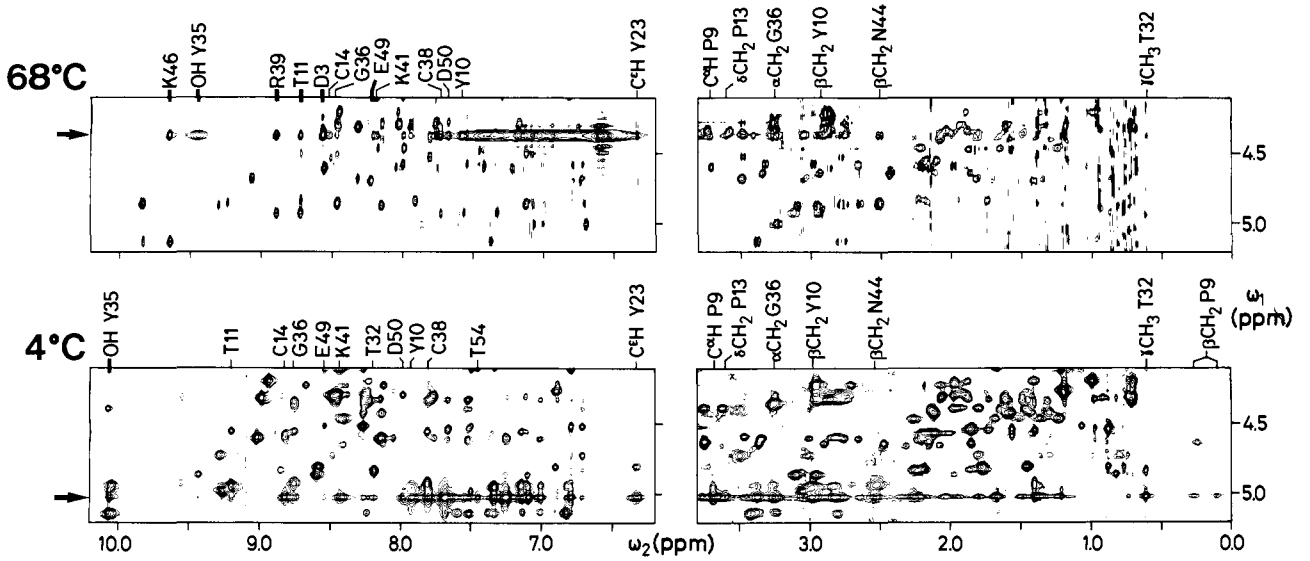

Figure 2. Spectral regions (ω_1 = 4.2–5.2 ppm, ω_2 = 0.0–3.8 ppm and 6.2–10.5 ppm) from contour plots of two NOESY spectra recorded at 600 MHz with a 15 mM solution of BPTI in 90% H_2O/10% ^2H_2O, 100 mM NaCl, pH 3.5, using the pulse sequence of Figure 1A with a mixing time of 112 ms. Arrows indicate the ω_1 frequency of the H_2O signal. NOE and exchange cross peaks with the water resonance are labeled above the spectra with the one-letter amino-acid symbol and the sequence position. Cross peaks due to chemical exchange are identified by the use of thicker lines, which are extended into the spectrum. The spectra were base-line corrected in both dimensions by using polynominals. Lower panel: spectrum at 4 °C, $t_{1_{max}}$ = 70 ms. Upper panel: spectrum at 68 °C, $t_{1_{max}}$ = 35 ms. Wiggles along ω_1 observed at the ω_2 position of the strongest peak arise from the truncation of the data set in t_1. At 68 °C the $C^\alpha H$–NH NOE cross peak of K46 overlaps with the exchange cross peak of K46 NH with the water (see text).

At 4 and 5 °C (Figures 2 and 3) the spectra contain a limited number of mostly well-separated cross peaks at the ω_1 frequency of the water. All NOESY cross peaks between protein resonances and the water signal that could be unambiguously assigned are labeled in Figure 2. Except for the cross peaks due to chemical exchange and the cross peaks with β-CH_2 of Pro-9, which probably arise from spin diffusion, all these peaks are manifested by negative ROESY cross peaks (Figure 3) and therefore come from direct NOE. Their intensity diminishes continuously with increasing temperature, but clearly there are still NOE cross peaks in the spectra at 68 °C. This is exemplified by the cross peak between the amide proton of Cys-14 and the water resonance, which is identified by an arrow in the ROESY spectra of Figure 3. In all, NOE cross peaks between protein protons and the water resonance position in NOESY and ROESY were identified for the amide protons of Tyr-10, Thr-11, Cys-14, Thr-32, Gly-36, Cys-38, Lys-41, Glu-49, Asp-50, and Thr-54, and for the nonexchangeable protons $C^\alpha H$ of Pro-9, β-CH_2 of Tyr-10, δ-CH_2 of Pro-13, $C^\epsilon H$ of Tyr-23, γ-CH_3 of Thr-32, α-CH_2 of Gly-36, and β-CH_2 of Asn-44.

As mentioned in the introduction, localization of oxygen atoms of hydration water molecules is usually part of a high-resolution protein crystal structure. For BPTI, structures have been determined at high resolution in three different crystal forms by X-ray crystallography and neutron diffraction,[3,29,30] and the structure determination by NMR has shown that the global molecular architecture in aqueous solution is the same as in these crystals.[31] In the three crystal forms, 60, 62, and 73 water molecules, respectively, have been located.[30] Sixteen water molecules were found to be in approximately the same locations in all three crystal forms, and 10 of these make the same hydrogen bonds. Four of these 10 fully conserved water molecules are located in the interior of the protein. They constitute an integral part of the protein structure and have no hydrogen bonds with hydration water on the protein surface. All other water molecules seen in the crystal structures are in the layer of hydration water on the protein surface.

In the crystal form II of BPTI, proton coordinates were determined by neutron diffraction.[29] Fifty-eight of the localized hydration water molecules have protons that are within a distance of ≤3.0 Å from protein protons, and there are about 240 water–proton to protein–proton distances within this range. A correspondingly large number of protein–H_2O NOEs would thus be expected. From the observations in Figures 2 and 3 it follows that of all the water molecules seen in the crystal structures, at most a small percentage gives rise to sizable negative NOEs with protein protons. In particular, all prominent NOE cross peaks with the water resonance, which could so far be assigned, can either be attributed to the four internal water molecules or could arise from side-chain hydroxyl protons as well as from hydration water protons. With the possible exception of a small number of discrete hydration sites, the first hydration sphere of BPTI in solution must therefore be kinetically highly labile.

The four internal water molecules in crystalline BPTI have been designated W111, W112, W113, and W122.[3,29,30] Among the protein protons seen in Figures 2 and 3 to have NOEs with the water resonance position, the amide protons of Cys-14, Gly-36, and Cys-38, and α-CH_2 of Gly-36 and δ-CH_2 of Pro-13 are all within 3.0 Å from the protons of the internal water molecule W122. Similarly, in the crystal structures the amide protons of Tyr-10 and Lys-41, $C^\alpha H$ of Pro-9, β-CH_2 of Tyr-10, and β-CH_2 of Asn-44 make contacts with one or two of the water molecules W111, W112, and W113 in the interior of the protein. Since no side-chain hydroxyls or carboxylates are close to any of these protein protons (a single exception is the amide proton of Gly-36, which is at a distance of 3.7 Å from the OH of Tyr-10 in the crystal structure[29]) and since these are also far from the protein surface, the NMR data present convincing evidence for the presence of the four internal water molecules also in the solution conformation of BPTI. The additional individually assigned NOEs from the amide protons of Thr-11, Thr-32, Glu-49, Asp-50, and Thr-54, $C^\epsilon H$ of Tyr-23, and γ-CH_3 of Thr-32 with the water resonance cannot be attributed unambiguously to intermolecular protein–water contacts, since all these protons are near neighbors of side-chain OH groups of either threonine, serine, or tyrosine. For all protons of hydration waters or OH groups of the protein, which are identified by positive NOESY cross peaks at 600 MHz, the lifetimes with respect to exchange with the bulk water must be longer than 3×10^{-10} s. This limit is obviously also valid for the lifetimes of the oxygen atoms of the same water molecules. Water molecules or OH groups of the protein that are not manifested by positive NOESY cross peaks have shorter proton-exchange lifetimes than 3×10^{-10} s (the oxygen atoms could of course have longer residence times).

In conclusion, NMR measurements using the experiments of Figure 1 at variable temperature over the range 4–68 °C provided

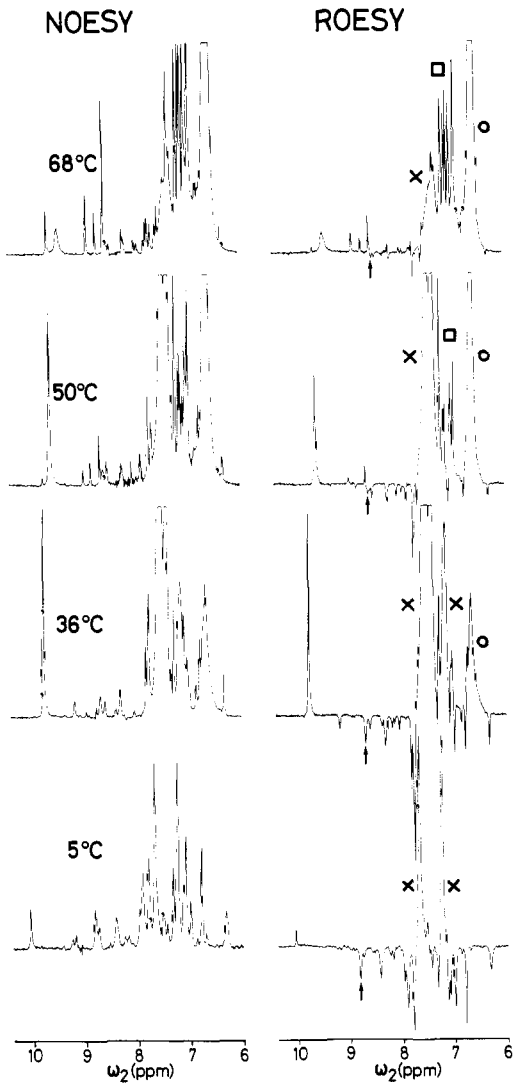

Figure 3. Corresponding cross sections parallel to the ω_2 axis taken at the ω_1 frequency of the water resonance in NOESY (left) and ROESY (right) spectra recorded at 5, 36, 50, and 68 °C. The NOESY spectra were recorded with a mixing time of 112 ms and the pulse sequence of Figure 1A. For the ROESY spectra the pulse sequence of Figure 1B was used with a mixing time of 87 ms. In the different ROESY cross sections, the NOE cross peak of the amide proton signal of Cys-14 with H_2O is identified with an arrow. Cross peaks with the water signal that manifest chemical exchange are identified in the ROESY cross sections with the following symbols: (×) Amino protons of lysine; (○, □) amino and imino protons, respectively, of the guanidinium group of arginine. With the exception of the NOESY cross section at 5 °C, where a reduced receiver gain setting was used, all cross sections are from spectra that were acquired and processed in an identical way.

unambiguous evidence that the four internal water molecules seen in the crystal structures of BPTI[3,29,30] are also an integral part of the solution conformation. Unambiguous evidence was further obtained for the presence of a discrete number of labile protons on the protein surface with lifetimes longer than 0.3 ns. It remains open if some or all of these protons correspond either to hydroxyl and carboxylate groups of the protein or to hydration waters. Compared to the corresponding crystal structures, the first hydration shell of BPTI in solution is clearly less well ordered. In particular, the present experiments show that the formation of a protein–water hydrogen-bonding network at the protein–water interface would, with the possible exception of a few unique sites, have to be very short-lived, with a lifetime shorter than 0.3 ns. This result is of special interest with respect to the indications obtained independently[8,31] that even when the core of a globular protein in aqueous solution is virtually identical with the corresponding crystal structure, the protein surface is generally more disordered in solution than in single crystals. Some of the questions raised by the present initial studies of protein hydration by high-resolution NMR may possibly be answered by rather straightforward further applications of the experiments in Figure 1. For example, measurements with other proteins than BPTI might reveal NOEs with protein surface groups that are sufficiently far apart from OH groups of the protein to produce unambiguous evidence for the presence of distinct molecules of hydration water on the protein surface. Also, studies of the influence of variable ionic strength, pH, etc. on the results obtained with these experiments might provide a wealth of additional insights relating to the characteristics of the interface between protein and solvent.

Experimental Section

Experiments were performed with the protein basic pancreatic trypsin inhibitor (BPTI). Material obtained from Bayer AG in Wuppertal, BRD (Trasylol) was used without further purification. For the NMR experiments we used a 15 mM solution of BPTI in a mixed solvent of 90% H_2O/10% ^2H_2O, containing 100 mM NaCl. A low pH value of 3.5 was chosen to be near the pH minimum for the rate of chemical exchange of labile protons from amide and guanidinium groups of the protein with the bulk water.[2]

The ^1H NMR experiments were recorded at 600 MHz on a Bruker AM 600 instrument. The following types of radio-frequency pulses were used in the experiments of Figure 1:

In ROESY a sequence of $\pi/4$ pulses was used as the mixing spin-lock.[23] To avoid TOCSY-type transfer of magnetization, the $\pi/4$ pulses were separated by delays 10 times longer than the width of the individual pulses.

The selective pulses applied to the water resonance during the mixing time in both NOESY and ROESY were Gaussian-shaped DANTE pulses consisting of a series of 32 pulses seperated by equal delays τ.[24-26] The shaping was achieved by increasing and decreasing the pulse lengths according to equidistant values on a Gaussian curve, starting at 1% of the maximum value. These Gaussian-shaped DANTE pulses are intrinsically very selective, but they exhibit additional excitation maxima at regular frequency intervals $1/\tau$. Therefore the delay τ must be chosen sufficiently short to place all excitation sidebands well outside of the spectrum. In practice, the pulse power was reduced by 27dB for the selective pulses relative to the nonselective pulses, and the shortest individual pulse used was longer than 0.2 μs. The exact length of these individual pulses was adjusted empirically to give the best water suppression. The optimum corresponded to a 70 or 80° pulse relative to a Gaussian pulse width corresponding to a 90° pulse. The 90° pulse width of the Gaussian pulse was determined by the maximum degree of water suppression in a two-pulse experiment, where a Gaussian pulse with phase x was immediately followed by a nonselective $(\pi/2)_{-x}$ pulse. The Gaussian-shaped DANTE pulses had a total length of 5 ms each and gave no significant excitation at 500 Hz away from the water signal. The suppression ratio was better than a factor 30 for a single scan at 4 °C, and appreciably higher suppression ratios resulted after completion of the phase cycle. The suppression efficiency was also increased at higher temperatures, where the water line is narrower, and could be further improved with the use of shorter, less selective Gaussian-shaped DANTE pulses with more pulse power.

Acknowledgment. We thank Bayer AG, Wuppertal, FRG, for a gift of BPTI (Trasylol), Dr. L. Orbons and Prof. G. Wagner for helpful discussions on the resonance assignment of BPTI, and R. Marani for the careful processing of the typescript. The pulse sequences with a homospoil pulse were tested at Spectrospin AG, Fällanden. Financial support by the Schweizerischer Nationalfonds (project 3.198.85) is gratefully acknowledged.